

Hammett Analyses of
Halocarbene—Halocarbanion Equilibria

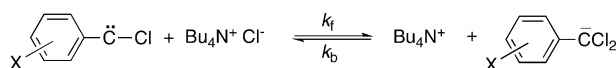
Lei Wang, Robert A. Moss,* and Karsten Krogh-Jespersen*

Department of Chemistry and Chemical Biology, Rutgers,
The State University of New Jersey, New Brunswick, New Jersey 08903, United States

moss@rutchem.rutgers.edu; krogh@rutchem.rutgers.edu

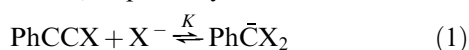
Received March 15, 2013

ABSTRACT

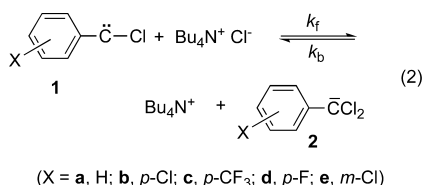


Substituted arylchlorocarbenes ($X = \text{H}$, $p\text{-Cl}$, $p\text{-CF}_3$, $p\text{-F}$, $m\text{-Cl}$) reacted reversibly with Cl^- in dichloroethane to form the corresponding aryldichloromethide carbanions. Equilibrium constants and rate constants for the forward and reverse reactions were correlated by the Hammett equation. DFT methods were used to compute equilibrium constants and electronic absorption spectra.

We reported a Hammett analysis of equilibrium constants for the formation of π -complexes between p -substituted arylchlorocarbenes and 1,3,5-trimethoxybenzene in pentane.¹ More recently, we spectroscopically characterized equilibria between phenylhalocarbenes, halide ions, and phenyldihalomethide carbanions; eq 1 ($X = \text{Cl}$ or Br). At 298 K, equilibrium constants were 4.01 or 3.01 M^{-1} for $X = \text{Cl}$ or Br , respectively.²



Herein we present a detailed Hammett study of equilibria between arylchlorocarbenes (**1**), chloride, and aryldichloromethide carbanions (**2**), eq 2.



We report σ/ρ correlations for K_{eq} , k_f , and k_b of eq 2 and for computed values of K_{eq} . The results reveal the sense and magnitude of the substituent electronic effects that operate in these equilibria. A previous study of k_f for eq 2 gave $\rho = +0.86$ for the capture of Cl^- by ArCCl .³

Carbenes **1a–1e** were generated by laser flash photolysis (LFP)⁴ of the corresponding diazirines in 1,2-dichloroethane (DCE) at temperatures ranging from 294 to 304 K. The diazirines were prepared by standard Graham oxidations of available⁵ or commercial amidines. In the presence of added tetrabutylammonium chloride (TBACl), LFP of the diazirines gave carbanions **2a–2e**, in addition to the carbenes.² The experimental absorption spectra were calibrated, and the corresponding spectra appear in the Supporting Information (SI).⁶ The experimental and principal computed absorption maxima of the carbenes and the carbanions are included in Table 1.⁷

Equilibrium constants for eq 2 were determined in DCE as described for **1a/2a** in ref 2. Consider, for example, the $p\text{-Cl}$ case, **1b/2b**. The ratio of the **1b** absorbance at 324 nm to the **2b** absorbance at 388 nm varied with [TBACl]: A_{324}/A_{388} decreased with the increasing concentration of TBACl.⁸

(4) We used a xenon fluoride excimer laser operating at 351 nm, emitting 42–56 ns pulses with 60–70 mJ power.

(5) Moss, R. A.; Terpinski, J.; Cox, D. P.; Denney, D. Z.; Krogh-Jespersen, K. *J. Am. Chem. Soc.* **1985**, *107*, 2743. Graham, W. H. *J. Am. Chem. Soc.* **1965**, *87*, 4396.

(6) Calibration corrects the intensities of the observed UV–vis absorptions for wavelength-dependent variations in sample absorptivity, xenon monitoring lamp emission, and detector sensitivity from 244 to 800 nm. Calibration curves appear in the SI.

(7) wB97XD/6-311+G(d) was used for calculation of ΔG and K in simulated dichloroethane. Excited state calculations (TD-B3LYP/6-311+G(d))/wB97XD/6-311+G(d)) in simulated dichloroethane produced absorption wavelengths and oscillator strengths (f). See SI for computational details.

(8) Each ratio remained constant from 150 to 200 ns after the laser flash (200–300 ns for **1c/2c**).

(1) Wang, L.; Moss, R. A.; Thompson, J.; Krogh-Jespersen, K. *Org. Lett.* **2011**, *13*, 1198.

(2) Wang, L.; Moss, R. A.; Krogh-Jespersen, K. *J. Am. Chem. Soc.* **2012**, *134*, 17459.

(3) Moss, R. A.; Tian, J. *Org. Lett.* **2006**, *8*, 1245.

Table 1. UV Absorptions of Carbenes **1** and Carbanions **2**^a

X	λ_{obsd}^b	λ_{calcd}^b	f^b	λ_{obsd}^c	λ_{calcd}^c	f^c
H	292	291	0.4770	404	393	0.1961
<i>p</i> -Cl	324	310	0.5454	388	396	0.2421
<i>p</i> -CF ₃	324	288	0.5254	388	397	0.2570
<i>p</i> -F	316	293	0.4874	388	388	0.1776
<i>m</i> -Cl	308	296	0.3880	388	393	0.2139

^a Reported in nm in DCE. Experimental absorbances are calibrated. See ref 7 for computational details. ^b Principal carbene absorptions. Only the strong $\pi \rightarrow p$ absorption is listed; weak $\sigma \rightarrow p$ carbene absorptions were observed at ~ 600 nm. ^c Principal carbanion absorptions.

Values of this ratio were determined over the 150–200 ns time interval as [TBACl] varied from 0.25 to 0.49 M; see the SI for the resulting LFP spectra. Beer–Lambert analysis of the data used computed oscillator strengths (f ; see Table 1)⁷ in place of the unknown extinction coefficients of **1b** and **2b**.^{9,10} A plot of A_{324}/A_{388} vs $1/[\text{TBACl}]$ gave a linear correlation (Figure S-17 in the SI), whose slope (0.072) led to $K = 31.3 (\pm 1.7) \text{ M}^{-1}$ for eq 2 when $X = p\text{-Cl}$.¹¹

Values of K were similarly determined for the other carbene/carbanion pairs; data for the unsubstituted **1a/2a** pair were taken from ref 2. Values of observed (K_{exp}) and calculated (K_{calcd}) equilibrium constants⁷ are collected in Table 2. These values are specific to DCE solution and ignore the possible aggregation of TBACl or the TBA salts of the carbanions.¹² We attempted to measure K for eq 2 with $X = p\text{-Me}$ or $p\text{-NO}_2$. However, with $p\text{-Me}$, K was too small and the carbanion absorbance (at 404 nm) was too weak for reliable measurement. With $p\text{-NO}_2$, K was too large and the carbene absorption (at 324 nm) could not be accurately measured; the carbanion appeared at 500 nm.

The kinetics of the forward process of eq 2 were followed by LFP, monitoring the apparent rate of formation of each carbanion as a function of [TBACl]. Rate constants (k_f) were obtained from the slopes of these correlations; see the SI.¹³ Values of k_b for the reverse process were obtained from the experimental data for K and k_f , according to $k_b = k_f/K$. The rate constants are collected in Table 2.

Hammett analyses were performed for K_{exp} , K_{calcd} , k_f , and k_b of Table 2. For K_{calcd} , in addition to the five cases

(9) Moss, R. A.; Wang, L.; Odorisio, C. M.; Krogh-Jespersen, K. *J. Am. Chem. Soc.* **2010**, *132*, 10677.

(10) Formally, the computed oscillator strengths are proportional to the frequency-integrated absorption coefficients. Although the widths of the carbene and carbanion absorption bands differ, we did not correct for this. We conservatively estimate that the $f_{\text{carbene}}/f_{\text{carbanion}}$ ratio accurately reproduces the desired $\epsilon_{\text{carbene}}/\epsilon_{\text{carbanion}}$ extinction constant ratio to within a factor of 2.

(11) $K = (\text{slope})^{-1}(f_2/f_1)$, where f_2 is the computed oscillator strength of the carbene and f_1 is the analogous factor for the carbanion. For **1b**, $f_2 = 0.5454$ at 324 nm and $f_1 = 0.2421$ at 388 nm (cf. Table 1).

(12) The computed and experimental K values clearly fall in the same order. Numerical differences may have arisen, because the calculations did not treat the dissolved ions in sufficient detail, ignoring *inter alia* cation–anion interactions between both TBA^+ and Cl^- , and TBA^+ and **2**.

(13) k_f values were redetermined in DCE. The values in ref 2 were measured in MeCN/THF or CCl_4 .

Table 2. Equilibrium and Kinetic Data for eq 2

X	$K_{\text{exp}} (\text{M}^{-1})^a$	$K_{\text{calcd}} (\text{M}^{-1})^a$	$10^{-8}k_f^b$	$10^{-7}k_b^c$
H	4.11	1.51×10^{-1}	1.97	4.91
<i>p</i> -Cl	31.3	5.00	3.16	1.01
<i>p</i> -CF ₃	242	8.76×10^4	5.19	0.215
<i>p</i> -F	3.04	6.91×10^{-2}	1.02	3.36
<i>m</i> -Cl	55.7	1.08×10^2	3.85	0.692

^a In DCE. ^b Rate constants in $\text{M}^{-1} \text{ s}^{-1}$. See SI for temperatures and errors. ^c In s^{-1} .

of Table 2, the computed values for eq 2 with $X = p\text{-NO}_2$, $p\text{-Me}$, and $p\text{-OMe}$ were included in the regression analysis.¹⁴ Hammett substituent constants were taken from Smith and March.¹⁵

First consider K_{exp} : inclusion of K for $X = \text{F}$ (**1d/2d**) is deleterious to the correlation. Omitting K_{exp} for $p\text{-F}$ leads to an excellent four-point correlation of $\log K$ vs σ_p , with $\rho = +3.26$ ($r = 0.995$); cf. Figure S-41. Inclusion of the $p\text{-F}$ point causes significant decay in the fitting: $\log K$ vs σ_p now gives $\rho = +3.67$ and r is reduced to 0.937; cf. Figure S-42. The positive values obtained for ρ imply that carbanion formation is favored by electron withdrawing substituents X , which destabilize carbene **1** but stabilize carbanion **2**. The $p\text{-F}$ substituent has $\sigma_p = +0.15$, indicating an electron withdrawing group that should enhance carbanion formation relative to H ($\sigma_p = 0$). However, the *computed* K_{calcd} values in Table 2 indicate that $p\text{-F}$ suppresses carbanion formation relative to H; $K_{\text{calcd}}(X = \text{F})/K_{\text{calcd}}(X = \text{H}) = 0.46$. In other words, $p\text{-F}$ acts as a net *donor* of electron density in eq 2; electron donation from a lone pair on F by resonance outweighs electron withdrawal by induction. Given that $p\text{-F}$ directly interacts with the carbene or carbanion center via the phenyl ring, σ_p^+ (−0.07) is a possible alternative for σ_p (+0.15) to represent $p\text{-F}$ in a Hammett analysis of eq 2.

Indeed, an excellent correlation of $\log K_{\text{exp}}$ vs σ is obtained using σ_p^+ for F (and σ_m for $m\text{-Cl}$); cf. Figure 1 where $\rho = +3.18$ ($r = 0.996$). Note, however, that using σ_p^+ also for $p\text{-Cl}$ leads to a decreased quality in the fit; $\rho = +3.01$, but r decreases to 0.959, Figure S-43.¹⁶

Using σ_p^+ for $p\text{-F}$, rather than σ_p , is one possible response to the computational results indicating that the $p\text{-F}$ substituent behaves as a net donor of electron density in eq 2. The use of σ_p^+ is similar to using σ_m for $m\text{-Cl}$. However, if a “pure” approach is preferred, one can simply accept the correlation with σ_p for $p\text{-F}$. The difference in ρ values (+3.18 with σ_p^+ vs +3.67 with σ_p) is neither very large nor mechanistically significant. In all the Hammett

(14) Calculated⁷ values of K for eq 2 with $X = p\text{-NO}_2$, $p\text{-Me}$, and $p\text{-OMe}$ are 1.46×10^{14} , 1.16×10^{-3} , and $4.24 \times 10^{-6} \text{ M}^{-1}$, respectively. See Table S-1 in the SI.

(15) Smith, M. B.; March, J. *March's Advanced Organic Chemistry, Reactions, Mechanisms, and Structure*, 6th ed.; Wiley: New York, 2007; p 404.

(16) The 3p–2p overlap of Cl with the *para* phenyl carbon atom is less efficient for transmission of electronic effects than the 2p–2p F–C overlap; hence, σ_p is more appropriate than σ_p^+ for the $p\text{-Cl}$ substituent.

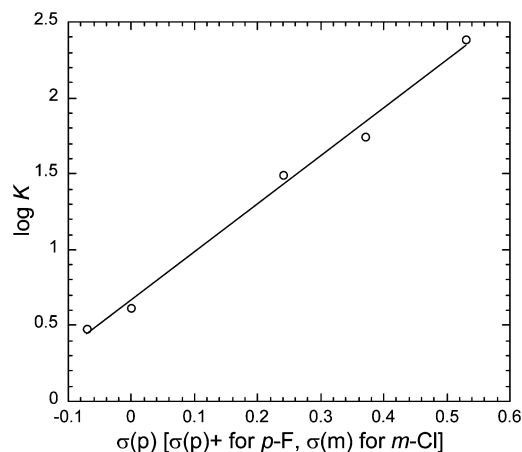


Figure 1. Hammett correlation of $\log K_{\text{exp}}$ vs σ_p [σ_p^+ for p -F, σ_m for m -Cl] for the equilibria of eq 2. See Table 2 and text: $\rho = +3.18$ ($r = 0.996$).

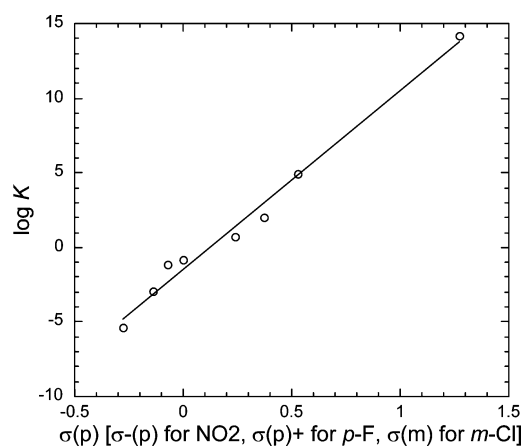


Figure 2. Hammett correlation of $\log K_{\text{calc}}$ vs σ_p [σ_p^- for p -NO₂, σ_p^+ for p -F, σ_m for m -Cl] for the equilibria of eq 2. See Table 2 and text: $\rho = +12.0$ ($r = 0.993$).

analyses, we present correlations that use σ_p^+ or σ_p for p -F. Again, the ρ values are comparable and the reader can weigh the benefits of the two approaches.

We also obtained an excellent correlation of the *computed* K values⁷ of Table 2 and ref 14; cf. Figure 2. Here we used σ_p^- for p -NO₂,³ σ_p^+ for p -F, σ_m for m -Cl, and σ_p for the other five substituents. We find $\rho = +12.0$ ($r = 0.993$). A comparably good fit was obtained using σ_p for p -F ($\rho = +12.3$, $r = 0.993$, Figure S-44), whereas using σ_p^+ for p -Cl and p -F led to some degradation in the fit ($\rho = +9.6$, $r = 0.977$, Figure S-45).

Why is ρ for K_{calc} (+12.0) so much higher than ρ for K_{exp} (+3.18)? The calculated K values refer to eq 2 with a full unit of negative charge on carbanion **2**, which will thus be very sensitive to electronic effects exerted by substituent X. However, in the experimental systems, cation/anion

interactions between Bu₄N⁺ and **2** will reduce the effective negative charge on the carbanion and mitigate the electronic effects wielded by X; accordingly, ρ will decrease. Possible aggregation of Bu₄N⁺ArCCl₂[−] could cause an additional dispersal of negative charge and further diminution of ρ .

The ρ values for the Hammett correlations of K_{exp} and K_{calc} are positive, indicating that eq 2 shifts toward the product carbanion (K increases) as X becomes more electron withdrawing, stabilizing the carbanion and destabilizing the carbene. An analogous ρ value (+2.48) was observed for the equilibrium between carbenes **1** and 1,3,5-trimethoxybenzene affording the corresponding π -complexes.²

A previous determination of k_f for eq 2 in MeCN–THF and CCl₄ solvents gave $\rho = +0.86$ ($r = 0.985$).³ A redetermination in DCE yields the data in Table 2. Omitting X = F leads to an excellent correlation vs σ_p (σ_m for m -Cl) with $\rho = +0.79$ ($r = 0.999$, Figure S-46). Inclusion of the point for X = F causes a very significant decay in fitting vs σ_p ($\rho = +1.06$, $r = 0.776$, Figure S-47). However, using σ_p^+ for p -F and σ_m for m -Cl, we obtain a reasonable correlation, Figure 3, where $\rho = +1.05$ ($r = 0.955$). If σ_p^+

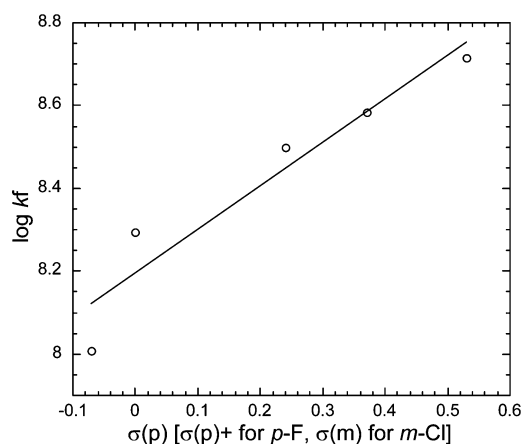


Figure 3. Hammett correlation of $\log k_f$ vs σ_p [σ_p^+ for p -F, σ_m for m -Cl] for the forward reaction of eq 2. See Table 2 and text: $\rho = +1.05$ ($r = 0.955$).

is used for all X (except m -Cl), the fit is poor with $\rho = +0.99$, $r = 0.906$, Figure S-48.

The ρ value for the forward process of eq 2 is positive; electron withdrawing groups that destabilize carbenes **1** and stabilize carbanions **2** accelerate the reaction. The magnitude of ρ (~ 0.8 – 1.0) is about a third of ρ for the equilibrium of eq 2, presumably because only a fraction of the unit negative charge imposed on the carbanion is present at the transition state of the forward reaction.

An excellent correlation is obtained for the k_b of the *reverse* reaction of eq 2, if X = F is omitted: a plot of $\log k_b$ vs σ_p (σ_m for m -Cl) gives $\rho = -2.49$, $r = 0.993$, Figure S-49. Inclusion of X = F affords a slightly poorer correlation with $\rho = -2.63$, $r = 0.979$, Figure 4. Use of σ_p^+ for

X = F yields a correlation of comparable quality with $\rho = -2.12$, $r = 0.973$, Figure S-50. Finally, a correlation with σ_p^+ for all points (except *m*-Cl) gives an inferior result; $\rho = -2.03$, $r = 0.943$, Figure S-51.

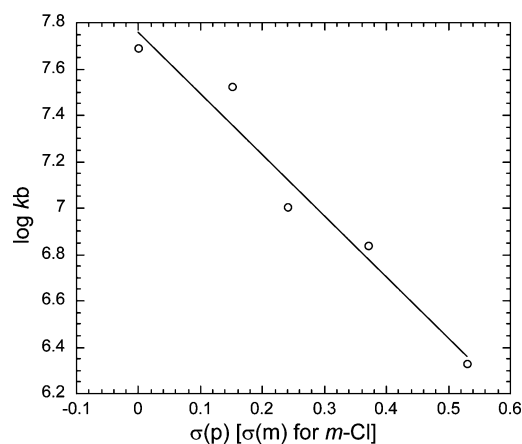


Figure 4. Hammett correlation of $\log k_b$ vs σ_p (σ_m for *m*-Cl) for the reverse reaction of eq 2. See Table 2 and text: $\rho = -2.63$ ($r = 0.979$).

The sign of ρ for the reverse reaction of eq 2 is negative, in contrast to the positive ρ for both the forward reaction

and the equilibrium. For the k_b process, electron donating groups destabilize the carbanion but stabilize the product carbene, accelerating the reaction and generating a negative ρ . The magnitude of ρ for k_b (~ 2.0 – 2.6) is about twice that of ρ for k_f . Presumably, the slower reverse reaction senses the transition state for eq 2 as being ‘later’ along the reaction coordinate than the faster forward reaction; hence the reverse reaction shows a greater sensitivity to the electronic effects of X.

In summary, substituted arylchlorocarbenes react with chloride reversibly to form the corresponding arylchloromethide carbanions. Experimental and computed equilibrium constants, as well as rate constants for the forward and reverse reactions, are correlated by the Hammett equation. The mechanistic implications of the resulting ρ values are analyzed.

Acknowledgment. We are grateful to the National Science Foundation for financial support.

Supporting Information Available. Figures S-1–S-51; computational details; computed thermodynamic parameters for eq 2 (Table S-1); computed geometries and energetics for carbenes and carbanions appearing in eq 2. This material is available free of charge via the Internet at <http://pubs.acs.org>.

The authors declare no competing financial interest.